

## Combined analysis of AMS-02 secondary-to-primary ratios: universality of cosmic-ray propagation and consistency of nuclear cross-sections

---

M. Vecchi,<sup>a,\*</sup> E. F. Bueno,<sup>a</sup> L. Derome,<sup>b</sup> Y. Génolini<sup>c</sup> and D. Maurin<sup>b</sup>

<sup>a</sup>*Kapteyn Astronomical Institute,*

*P.O. Box 800, 9700 AV Groningen, The Netherlands*

<sup>b</sup>*LPSC, Université Grenoble Alpes,*

*CNRS/IN2P3, 53 avenue des Martyrs, 38026 Grenoble, France*

<sup>c</sup>*Niels Bohr International Academy Discovery Center,*

*Niels Bohr Institute, University of Copenhagen, Blegdamsvej 17, DK-2100 Copenhagen, Denmark*

*E-mail: [m.vecchi@rug.nl](mailto:m.vecchi@rug.nl)*

The AMS-02 collaboration released several secondary-to-primary ratios of unprecedented accuracy. These ratios can be used to test the universality of propagation for different species, and also to test the presence of breaks in the diffusion coefficient. It was shown in Weinrich et al. (AA 639, 131, 2020) that the combined analysis of Li/C, Be/C, and B/C strengthens the case for a low-rigidity diffusion break. It was also shown that a standard propagation model successfully reproduces these ratios (and also AMS-02 N/O and 3He/4He data), without the need for additional sources of Li, Be, or B. However, significant modifications (10-15%) of the production cross-sections are required, though these modifications remain within estimated nuclear uncertainties. We also extend our analyses to the recently published F/Si ratio and discuss how much F at the source can be accommodated by the data.

*37<sup>th</sup> International Cosmic Ray Conference (ICRC 2021)*

*July 12th – 23rd, 2021*

*Online – Berlin, Germany*

---

\*Presenter

## 1. Introduction

The AMS-02 collaboration, on the International Space Station since 2011, continues expanding the body of high-precision galactic cosmic-ray (CR) data [1]. In particular, AMS-02 provides elemental fluxes and ratios with high precision from 1 GV to a few TV in rigidity ( $R = pc/Z$ ). These data challenge the standard picture of CR transport in the Galaxy [2]. We study whether the recent measurements of F/Si [3] by the AMS-02 Collaboration can be reproduced by propagation models tuned on lighter secondary-to-primary ratios (Li/C, Be/C, B/C), and how much F at source can be accommodated by the data.

This work is organised as follows: in section 2 we give a short description of the general framework used for our study, while in section 3 we discuss the methods used in this analysis and in section 4 we present our findings concerning the production of cosmic-ray fluorine. In section 5 we present our results, while in 6 we present our conclusions.

## 2. Cosmic-ray propagation in the galaxy

In this section, we introduce the transport equation that we solve semi-analytically with the USINE code [4]. The general formalism that describes the CR transport in the galaxy [5] relies on the following diffusion-advection equation for a CR species of index  $\alpha$ , extensively discussed in [6]. In the steady-state approximation and in energy space (rather than rigidity or momentum space) the transport equation reads:

$$-\mathbf{x} \cdot \left\{ K(E) \vec{\nabla}_{\mathbf{x}} \psi_{\alpha} - \vec{V}_c \psi_{\alpha} \right\} + E \left\{ b_{\text{tot}}(E) \psi_{\alpha} - \beta^2 K_{pp} \psi_{\alpha} E \right\} + \sigma_{\alpha} v_{\alpha} n_{\text{ism}} \psi_{\alpha} + \Gamma_{\alpha} \psi_{\alpha} = q_{\alpha} + \sum_{\beta} \left\{ \sigma_{\beta \rightarrow \alpha} v_{\beta} n_{\text{ism}} + \Gamma_{\beta \rightarrow \alpha} \right\} \psi_{\beta} .$$

This equation describes the spatial and energy evolution of the differential interstellar CR density per unit energy  $\psi_{\alpha} \equiv dn_{\alpha}/dE$ , assuming a net primary injection rate of  $q_{\alpha}$ , and a secondary injection rate arising from inelastic processes converting heavier species of index  $\beta$  into  $\alpha$  species (with a production rate  $\sigma_{\beta \rightarrow \alpha} v_{\beta} n_{\text{ism}}$  on the ISM density  $n_{\text{ism}}$ , or a decay rate  $\Gamma_{\beta \rightarrow \alpha}$ ). This source term is balanced by several other terms, among which the decay rate  $\Gamma_{\alpha}$  (if relevant). The central piece of the propagation equation is the spatial diffusion coefficient  $K$ , which we discuss in more detail in the following. The other processes are most relevant at low rigidity, but may still affect the determination of higher-energy parameters: convection is described by a velocity  $\vec{V}_c$ , diffusive reacceleration is described by the energy-dependent coefficient  $K_{pp}$ , and the inelastic destruction rate is expressed by  $\sigma_{\alpha} v_{\alpha} n_{\text{ism}} \psi_{\alpha}$ , with the  $\sigma$ 's being energy-dependent nuclear cross-sections; energy losses are characterised by the rate  $b_{\text{tot}} \equiv dE/dt$ , which includes ionisation and Coulomb processes as well as adiabatic losses induced by convection and reacceleration. We assume a 1D propagation model, where the magnetic halo confining the CRs is an infinite slab in the radial direction and of half-height  $L$ , whose value is fixed to 5 kpc, and was found to have a negligible impact on the results. In this frame, the vertical coordinate  $z$  is the only relevant spatial coordinate, and the galactic disk, where the sources of CRs as well as the interstellar medium gas lie has an effective half-height  $h = 100 pc$ ; the observer is located at  $z = 0$ .

The source spectrum  $q_\alpha$  is described by means of a single power law in rigidity. The diffusion coefficient is a key physical ingredient to describe CR transport. It describes the scattering of CRs off magnetic turbulence. It depends on the rigidity, and we assume that it can be described as a scalar function, homogeneous and isotropic all over the magnetic slab. In this work we use the general form presented in [6], which features a break in both the low and high-rigidity range:

$$K(R) = \underbrace{\beta^\eta}_{\text{non-relativistic regime}} K_0 \underbrace{\left\{ 1 + \left( \frac{R}{R_1} \right)^{\frac{\delta_1 - \delta}{s_1}} \right\}^{s_1}}_{\text{low-rigidity regime}} \underbrace{\left\{ \frac{R}{(R_{10} \equiv 10 \text{ GV})} \right\}^\delta}_{\text{intermediate regime}} \underbrace{\left\{ 1 + \left( \frac{R}{R_h} \right)^{\frac{\delta - \delta_h}{s_h}} \right\}^{-s_h}}_{\text{high-rigidity regime}} .$$

This equation couples about a hundred CR species (for  $Z < 30$ ) over a nuclear network of more than a thousand reactions. To solve this diagonal matrix of equations, we start with the heaviest nucleus, which is always assumed to be a primary species, and then proceed down to the lightest one.

We use the SLIM propagation scenario, initially proposed in [6], in which the low energy effects, convection and reacceleration, are discarded. We have 4 free propagation parameters, namely the normalisation of the diffusion coefficient  $K_0$ , the diffusion coefficient for intermediate rigidities  $\delta$ , and the low-rigidity parameters  $\delta_1$  and  $R_1$ .

### 3. Methodology

In order to reduce biases in the transport parameter determination, it is crucial to use nuisance parameters for the nuclear production cross-sections, and a covariance matrix for the data systematic uncertainties, as described in [7]. Fluxes calculated from the transport equation correspond to Interstellar fluxes (IS). They are modulated with the force-field approximation, which has the Fisk potential  $\Phi$  as a nuisance parameter. The average value of the Fisk potential is obtained from Neutron Monitor data following the method described in [8]<sup>1</sup>. The resulting top-of-atmosphere (TOA) fluxes are then compared to data, and we perform a  $\chi^2$  minimisation, with four free propagation parameters, one source free parameter and the Fisk potential and two cross-section normalisations (production and destruction) as nuisance parameters.

### 4. Production of cosmic-ray fluorine

Cosmic-ray fluorine is thought to be mostly of secondary origin, and it is purely composed of  $^{19}\text{F}$ . Following the methodology proposed in [9], we identify and rank the most important channels contributing to the secondary production of  $^{19}\text{F}$ , both from single and successive fragmentation processes.

The results are shown in Fig. 1. The left plot shows that Ne, Mg, Si and Fe are the main progenitors of F, while the right plot shows the individual contribution per process. We have identified 35 channels whose individual contribution is in the range [0.1-2%] and contribute to 22% of the total. Three channels dominate the total production of F,  $^{20}\text{Ne} \rightarrow ^{19}\text{F}$  (40%),  $^{24}\text{Mg} \rightarrow ^{19}\text{F}$  ( $\sim 12\%$ ) and  $^{28}\text{Si} \rightarrow ^{19}\text{F}$  ( $\sim 11\%$ ) contributing to 60% of the total.

<sup>1</sup>Retrieved from the Cosmic Ray Database <https://lpsc.in2p3.fr/crdb/>

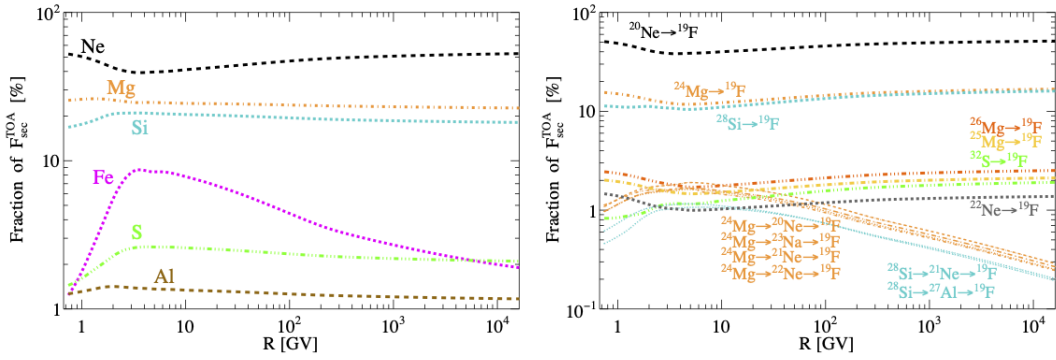


**Figure 1:** Dominant contributors of the total F production (modulated at 700 MV) as a function of rigidity. The left panel shows the dominant progenitors, while right panel shows the dominant channels (reactions paths). In both plots, contributions from different elements are colour coded. In the right panel, we further use different shades of the same colour to identify different isotopes of the same element.

These numbers were calculated using isotopic source abundances fixed to their Solar system fractions, i.e. not fit to isotopic galactic CR data. While the ranking of the dominant channels is a robust prediction, the individual numbers are subject to uncertainties due to the cross-section and propagation parameters.

Cross-section uncertainties can be sizeable (up to 20%) and must be accounted for in the modelling. Given the large network of reactions, the difficulty to assess the uncertainty on a reaction-to-reaction basis, and the similar impact different reactions have on the quantity of interest (e.g. F/Si), we pick a few reactions only as proxies for the whole network.

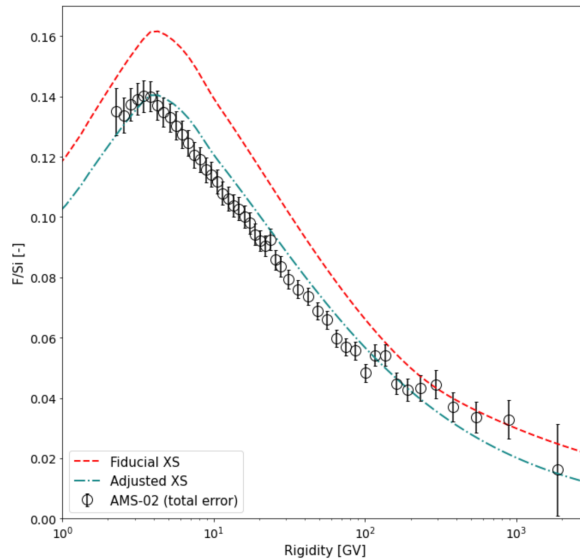


**Figure 2:** F/Si as a function of rigidity, for both AMS data [3] and theoretical predictions. The red dashed curve shows the model obtained using the propagation parameters from [10]. The green dot-dashed curve indicates the result of a fit with the fluorine production cross-section normalisation as a free parameter.

## 5. Results

The red curve in Fig. 2 shows that the model tuned on light nuclei AMS-02 data [10] overshoots F/Si data by 10% - 15% similar to the findings of [11]. The green dot-dashed curve indicates the model obtained using the same propagation parameters but leaving the production cross-section normalisation as a free parameter. A reduction of about 15% in the XS normalisation is needed to recover the difference, in the range of expected XS uncertainties. Fig. 3 shows our results of the

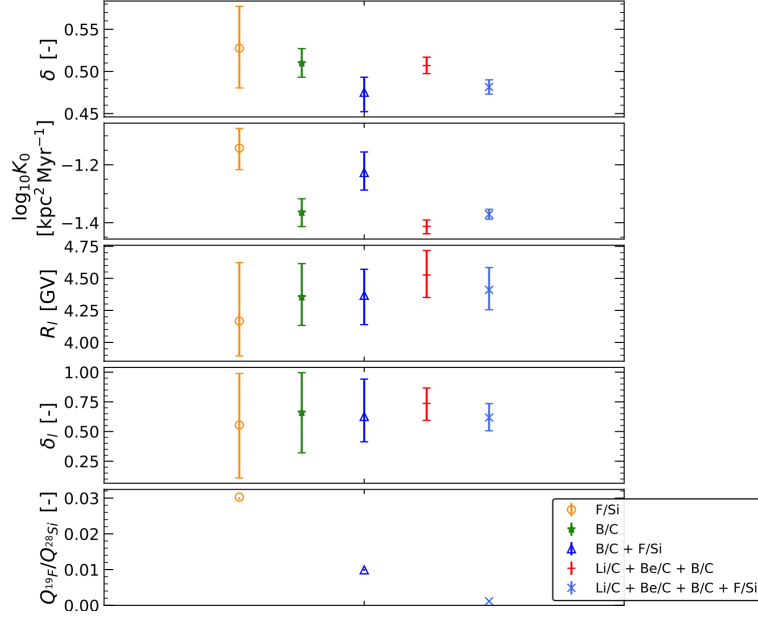


**Figure 3:** Results of the  $\chi^2$  minimisation, with four free propagation parameters, one source free parameter and the Fisk potential and two cross-section (production and destruction) as nuisance parameters. From top to bottom the parameters are:  $\delta$ ,  $\log_{10}K_0$ ,  $R_l$ ,  $\delta_l$ ,  $\frac{Q_{19F}}{Q_{28Si}}$ . The five data point per panel correspond to the five data sets used for the fit.

$\chi^2$  minimisation, with four free propagation parameters, one source free parameter and the Fisk potential and two cross-section (production and destruction) as nuisance parameters. From top to bottom the parameters are:  $\delta$ ,  $\log_{10}K_0$ ,  $R_l$ ,  $\delta_l$ ,  $\frac{Q_{19F}}{Q_{28Si}}$ . The five data point per panel correspond to the five data sets used for the fit (see legend). We see that the five cases provide results in good agreements for the four propagation parameters, even if for  $K_0$  only a marginal agreement is achieved, possibly due to the cross-sections. The last panel shows the fluorine source abundance, relative to  $^{28}Si$ : the constraints on this latter parameter depend strongly on the data set used for the fit. When performing a combined fit of F/Si and lighter CR species. we obtain an upper limit on the fluorine abundance.

## 6. Conclusions

Using the propagation parameters which give the best fit of lighter secondary-to-primary ratios, our preliminary results indicate that the model overestimates the data by 10% - 15%. However, this difference can be explained by the F production cross-sections uncertainties. We conclude that

all secondary species from Li to F can be explained by the same transport parameters. Combined analysis of Li/C, Be/C, B/C and F/Si gives an upper limit on the F source abundance, that can provide useful implications towards the understanding of stellar nucleosynthesis.

## References

- [1] M. Aguilar *et al.* [AMS], Phys. Rept. **894** (2021), 1-116
- [2] L. O. Drury and A. W. Strong, Astron. Astrophys. **597** (2017), A117
- [3] M. Aguilar *et al.* [AMS], Phys. Rev. Lett. **126** (2021) no.8, 081102
- [4] D. Maurin, Comput. Phys. Commun. **247** (2020), 106942
- [5] E. Amato and P. Blasi, Adv. Space Res. **62** (2018) 2731
- [6] Y. Génolini, M. Boudaud, P. I. Batista, S. Caroff, L. Derome, J. Lavalley, A. Marcowith, D. Maurin, V. Poireau and V. Poulin, *et al.* Phys. Rev. D **99** (2019) no.12, 123028
- [7] L. Derome, D. Maurin, P. Salati, M. Boudaud, Y. Génolini and P. Kunzé, Astron. Astrophys. **627** (2019), A158
- [8] A. Ghelfi, D. Maurin, A. Cheminet, L. Derome, G. Hubert and F. Melot, Adv. Space Res. **60** (2017), 833-847
- [9] Y. Genolini, D. Maurin, I. V. Moskalenko and M. Unger, Phys. Rev. C **98** (2018) no.3, 034611
- [10] N. Weinrich, Y. Génolini, M. Boudaud, L. Derome and D. Maurin, Astron. Astrophys. **639** (2020), A131
- [11] M. J. Boschini, S. Della Torre, M. Gervasi, D. Grandi, G. Johannesson, G. La Vacca, N. Masi, I. V. Moskalenko, S. Pensotti and T. A. Porter, *et al.* [arXiv:2106.01626 [astro-ph.HE]].